Generation and Propagation of Intense Supersonic Beams

ARTICLE *in* THE JOURNAL OF PHYSICAL CHEMISTRY A · JUNE 2011

Impact Factor: 2.69 · DOI: 10.1021/jp201342u · Source: PubMed

3 AUTHORS, INCLUDING:

Wolfgang Christen
Humboldt-Universität zu Berlin
31 PUBLICATIONS **398** CITATIONS
SEE PROFILE

Uzi Even
Tel Aviv University
176 PUBLICATIONS **5,367** CITATIONS
SEE PROFILE

THE JOURNAL OF PHYSICAL CHEMISTRY A

ARTICLE

pubs.acs.org/JPCA

Generation and Propagation of Intense Supersonic Beams

K. Luria,[†] W. Christen,[‡] and U. Even*[,†]

[†]Sackler School of Chemistry, Tel Aviv University, Tel Aviv, Israel

[‡]Humboldt-Universität zu Berlin, Institut für Chemie, Berlin, Germany

ABSTRACT: Computer simulations and experiments have been performed to quantify the effects of nozzle shape and skimmer placement on high-density supersonic jets. It is shown that the on axis beam intensity achieved is much higher than intensity achieved using standard sonic nozzles. Changes in skimmer design and positioning are required to allow this intense jet to propagate in a typical supersonic beam setup.

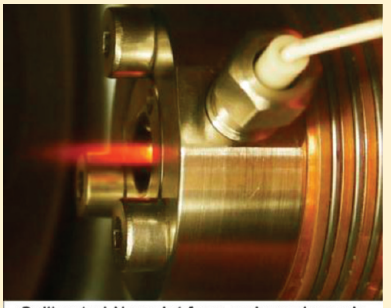

Collimated Neon jet from a shaped nozzle

I. INTRODUCTION

Molecular beams, and later, supersonic beams, have played a major role in chemical physics research for almost a century.[1] Due to significant technological improvements, the field has progressed as several recent textbooks prove.[2−4] If at the early stage small diameters (<0.1 mm), low source pressures (p < 10 bar), and CW pinhole nozzles were the norm,[5−8] the invention of pulsed valves enabled a remarkable increase in achieved beam intensity while maintaining the same required pumping capacity.[9−12] Nozzle shape[13−16] and skimmer geometry[17−20] were recognized as crucial elements in determining beam properties. Recent development of fast acting valves,[21,22] with opening times of 20 μs, enabled the use of even higher pressures. Improvement in beam cooling[23−25] and directionality[26] resulted in derived higher beam intensities. We combine beam flow simulation of nozzles and skimmers and actual measurements to emphasize the importance of nozzle shape and skimmer placement.

II. NOZZLE FLOW SIMULATION

The flow of gas in a nozzle can now be handled on a PC by using the highly evolved, freely available, direct simulation Monte Carlo program written by G. Bird.[27] "The simulation technique is modeling a real gas by millions of simulated molecules. The velocity components and position coordinates of these molecules are stored in the computer and are modified with time as the molecules are followed through representative collisions and boundary interactions. A statistical approach for the collision pair is used instead of solving the Navier-Stokes equation".[27] This program can now handle flows also at very low Knudsen numbers (K_n = mean free path/flow dimension < 0.001), as is explained in ref 28. The current limit, set by a single processor computation speed, seems to be a pressure of one bar for a few mm nozzle dimensions. This limit is much lower than the actual pressures used in pulsed nozzles (10−100 bar), but for hard sphere systems, the mean free path is much lower than the nozzle dimensions and the flow did not change drastically when we increased the simulated pressure from 0.1 to 0.3 bar. We limit our calculations to helium flows, as the program does not handle the formation of clusters that occur in heavier gas expansions. Comparison with actual measurements confirms this assumption. The basis for comparison is a simple pinhole nozzle (0.2 mm opening and 0.2 mm length, Figure 1), fed by helium gas at room temperature and 0.1 bar, expanding into a perfect vacuum. This simple nozzle flow can also be solved using classical fluid hydrodynamics, and the results obtained by the simulation here are comparable (in density and temperature maps).

The simulation provides much more information. Parameters like the temperature map (4 K at a distance of 5 mm), mean free path (4 mm at this distance), and angular beam spread are obtained. Beam spread is defined as the full angular width of the beam at half its maximum on axis value. For sonic nozzle this beam spread is 1 Steradians. The radial expansion from a pinhole nozzle is not confined by nozzle walls and accounts for the rapid density decrease of the beam (dropping by 4000 at 25 nozzle diameters) and fast cooling.

The wide beam spread (fwhm of 1 Steradians) for a sonic nozzle can be controlled by shaping the nozzle. We tested many nozzle shapes and present here detailed data for a family of conical nozzles, with a length of 10 nozzle diameters (2 mm) and variable cone angles. An example is a 50° full angle nozzle presented in Figure 2. All simulations presented here are for 0.1 bar of helium from nozzles of 0.2 mm opening.

Special Issue: J. Peter Toennies Festschrift

Received: February 10, 2011
Revised: March 29, 2011
Published: April 12, 2011

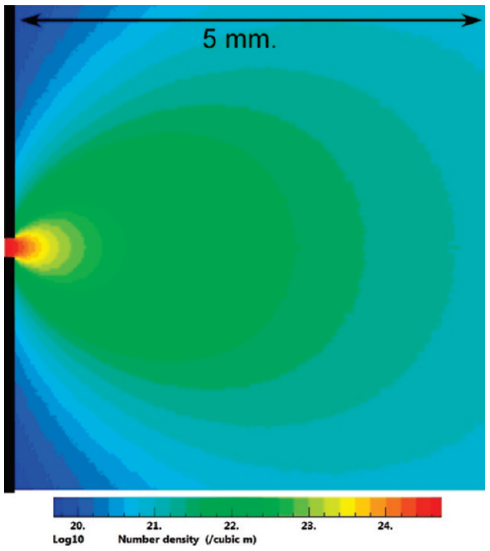

Figure 1. Density contours of helium expanding from a 0.2 mm sonic nozzle.

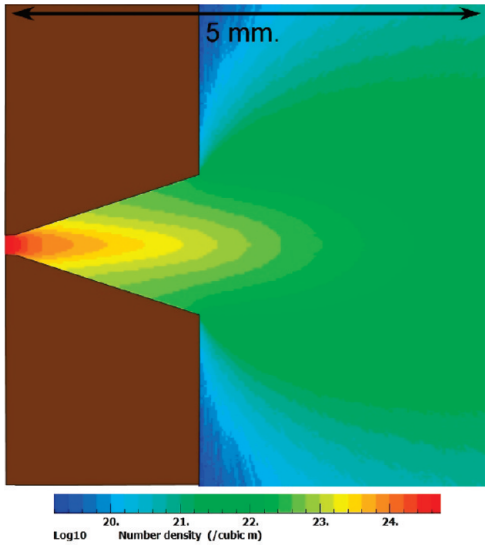

Figure 2. Density map for a conical 0.2 mm nozzle.

Figure 2 is a density map showing the simulation of a jet expanding from a 0.2 mm, 40° (full angle) conical nozzle. The length scale is 5 mm. The stagnation gas density is equivalent to 0.1 bar at room temperature, dropping by a factor of 700 over a distance of 25 nozzle diameters (a factor of six higher densities over that obtained for a sonic nozzle). The temperature is 15 K at this distance (compared to 4 K in the sonic nozzle), and the angular beam spread (fwhm) is now only 0.43 Steradians. This lower divergence will be advantageous (producing higher beam densities) at longer working distances (when using a skimmer for instance). A comparison of the density axial density drop with distance is shown in Figure 3 for two conical nozzles (40 and 70° full angle) and the simulated temperature drop is shown in Figure 4. Note the reheating of the gas in the nozzle as reflected shock waves from the boundaries interact with the expansion.

Figures 5 and 6 show the simulated beam spread and the expected beam density at a stagnation pressure of 30 bar and at a

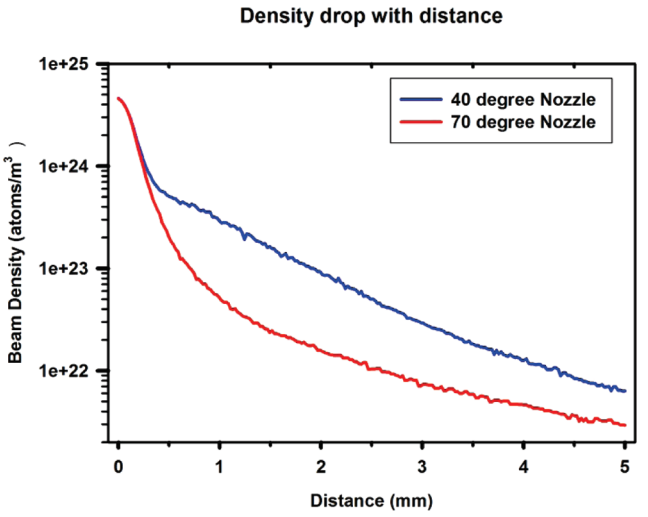

Figure 3. Simulated number density, shown as a function of distance, for two conical nozzles. A slower drop with distance is achieved for a 40° (full angle) nozzle.

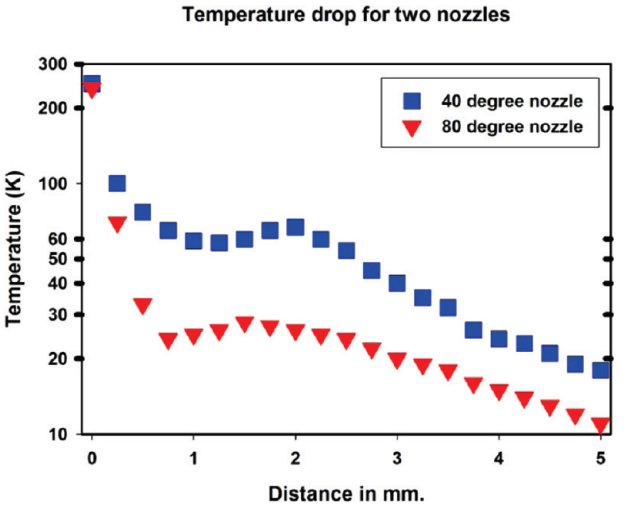

Figure 4. Simulated translation temperature drop for two conical nozzles. The confinement of the jet expansion and the interaction with the walls in the nozzle arrests the cooling in the jet (nozzle length is 2 mm). The simulation assumes full energy and momentum accommodation of the collision with the wall, creating a boundary layer of hotter gas. The lower confinement for the 80° nozzle causes a more rapid temperature drop.

distance of 1000 nozzle diameters (200 mm) and various nozzle opening (full) angles.

We can summarize the performance of conical nozzles according to several parameters, as shown in Table 1. The last column was obtained by multiplying the gas density at the nozzle exit by 300 (from the simulated value obtained for 0.1−30 bar) and using the fwhm beam angular spread from the simulation to calculate the extrapolated axial beam density at 200 mm.

The last column estimates the beam number density at a distance of 1000 nozzle diameters (200 mm from the nozzle!) when the nozzle is operated at 30 bar, while taking into account the simulated beam spread. The beam density is so high, even at these large distances, that skimmer interference can be a dominant

dx.doi.org/10.1021/jp201342u |J. Phys. Chem. A 2011, 115, 7362–7367

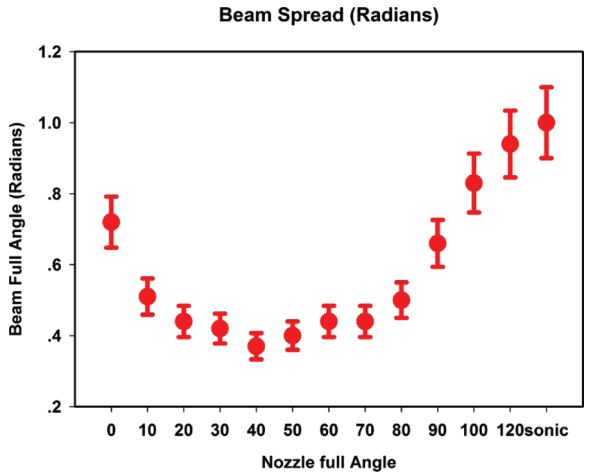

Figure 5. Simulated beam spread (fwhm density in Radians) for various nozzle openings.

Table 1. Beam Density Comparison of Conical Nozzles

nozzle opening angle (°)	simulated axial beam density at 25 nozzle diameters (atoms/m^3)	beam spread (fwhm in Steradians)	extrapolated beam density at a distance of 1000 nozzle diameters (atoms/m^3) and 30 bar
0	3.0e21	0.54	3.5e21
10	4.4e21	0.51	1.2e22
20	4.9e+21	0.49	1.6e22
40	6. e+21	0.43	2.0e22
50	7.2e+21	0.46	2.5e22
60	7.1e+21	0.44	2.3e22
80	4.6e+21	0.52	1.1e22
90	3.3e21	0.60	4.5e21
100	2.2e+21	0.83	1.9e21

mechanism in beam transfer[5,19] as will be discussed later. The beam angular spread produced by the nozzle depends on the detailed model for the gas surface interaction. The presented results so far assumed a full accommodation of the atom energy on collision with the surface. A partial accommodation model was also tried,[29] and the results were similar (with even a more pronounced beam collimation effects).

III. COMPARISON WITH EXPERIMENTAL NOZZLES

We measured the angular distribution of the jet produced by an 0.2 mm, 40° conical nozzle at 50 bar of helium and compared it to a sonic nozzle of similar opening. A fast ion gauge measured the (relative) beam intensity as we rotated the nozzle.[26] The results are presented in Figure 7. The measurements confirm our simulation results. A large forward intensity increase in the case of the conical 40° nozzle, with a beam spread of about 0.3 Steradians. A visual presentation of a glowing neon gas is shown in Figure 8. The gas is excited by dielectric barrier discharge,[22] producing a cold plasma. The measured angular beam spread is only 0.3 Steradians (while the simulations predicted value was 0.43 Steradians). The increase in on axis measured beam intensity is 20 times that of the sonic nozzle, while

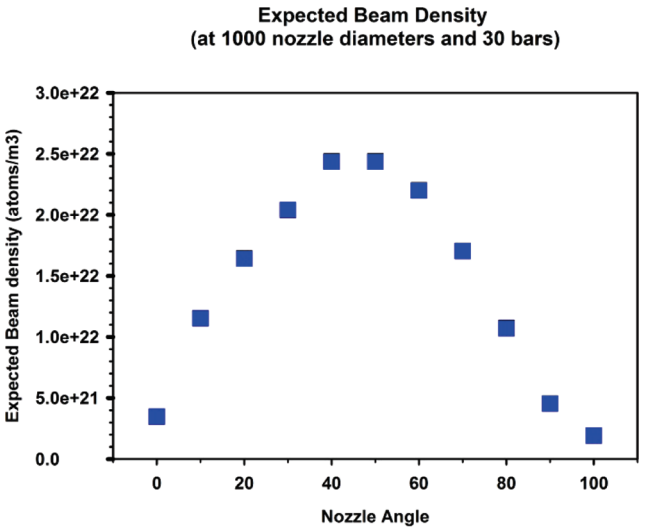

Figure 6. Extrapolated beam density for various nozzle angles. Nozzles of 40−50° opening produces the largest beam density and smallest beam divergence.

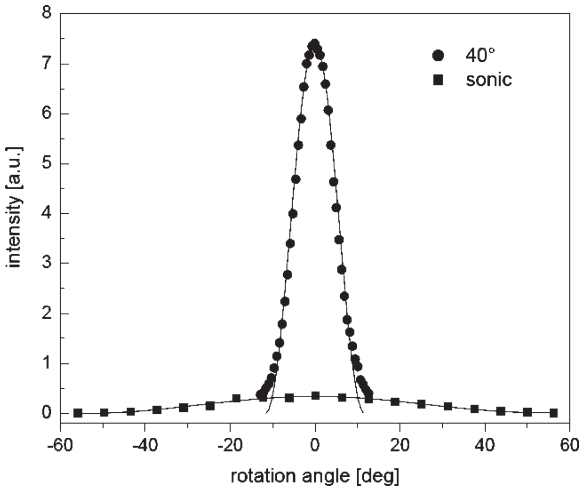

Figure 7. Measured beam intensity for a sonic and conical nozzle of 0.2 mm of helium expanded at 50 bar.

the simulations show an increase by a factor of 10. The difference between the simulations, and measured performances may be accounted for by the modeling of the helium interaction with the nozzle surface in the simulations. We used a full accommodation model (that is the reflected atoms are leaving the surface), with the velocity determined by the surface temperature only. Accommodation factor smaller than 1 has been reported.[29] A smaller accommodation coefficient will result in a smaller beam spread and, therefore, higher on axis beam density.

IV. BEAM PROPAGATION AND SKIMMER INTERFERENCE

In many cases, we use supersonic beams in a differentially pumped two chamber setup separated by a skimmer. Skimmers are not a neutral device letting the central part of the beam path unhindered. It is well-known that "skimmer interference" degrades the beam (in temperature, intensity, and angular spread)

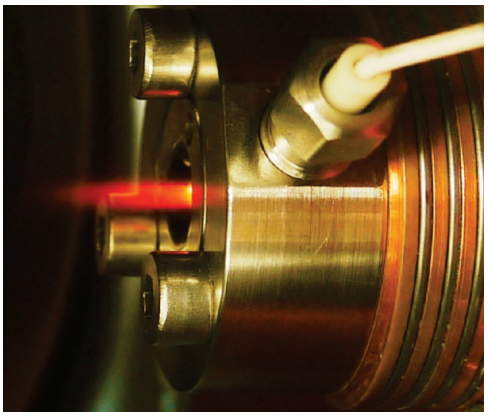

Figure 8. Neon jet from a 40° conical nozzle. The neon glows by a pulsed electrical discharge in the nozzle.

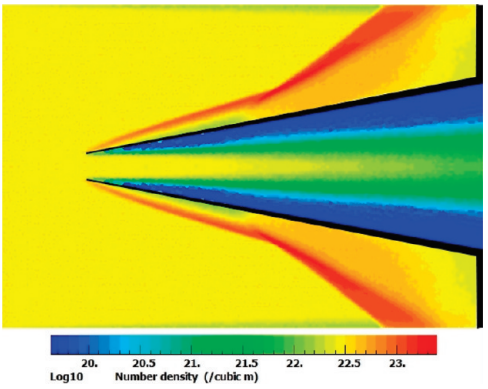

Figure 9. Density map of a CW flow around a slim skimmer with large opening.

and, in some extreme cases, can block the beam completely.[14,18,19,30] Most studies in the past of the skimmer effects were dedicated to continuous beams, and the findings (skimmer shape and placement) were copied to the pulsed beams without changes. There are several major differences between a pulsed beam propagating through a skimmer and a CW beam. The first point is that the background pressure during the pulse is low enough to move the bow shock wave (zone of silence[5]) to many cm from the nozzle. The second point is that pulsed beams are usually colder (1 K) than a CW beam (5 K) because the restriction of limited pumping is removed and higher flows can be obtained.[31] Thus, the radial velocity component of atoms is lower in the pulsed case (~100 m/s for helium). The short duration of the pulsed beam (that reaches 30 μs for a helium pulse at the skimmer inlet, 200 mm from the nozzle) limits the distances to the surfaces that are involved in the skimmer interaction, to a few (3) mm in the radial direction. There is no time for a pressure to build up inside the skimmer. Thus, slim skimmers (that remove the shock wave from the skimmer tip) can be used more freely. The DSMC program is ideally suited to visualize the flow in the regime of the extrapolated densities from a shaped nozzle. Figure 9 shows the flow of a 1 K helium beam moving at 1750 m/s and a beam density of 3×10^{22} atoms/m^3. The grid used for the simulation is fine enough to allow a skimmer tip definition of 3 μm only. Skimmer angle is 25° (total), length is 50 mm, and its opening diameter is 3 mm. The shock wave is weak at the tip, but the gas is still heated as can be seen in

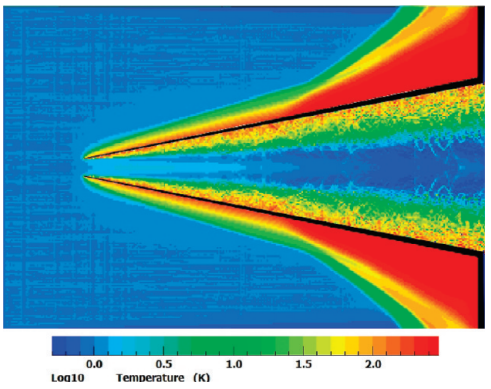

Figure 10. Translation temperature map (logarithmic scale) of a CW flow for a slim skimmer.

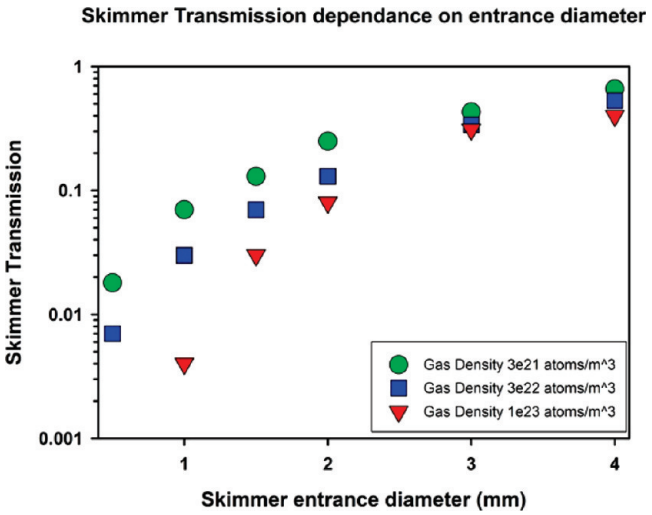

Figure 11. Skimmer transmittance for several openings and beam densities.

Figure 10. The local hot spot (2 K in this case), formed near the skimmer inlet, causes the gas to expand radially at an angle of 0.1 Steradians, lowering the axial beam density as it leaves the skimmer base. The simulation allows us to plot the axial beam density attenuation as a function of skimmer opening, as shown in Figure 11.

We could simulate and quantify the beam blocking occurring in small skimmer entrance diameters and large incoming beam densities. Even at large diameters (4 mm), skimmer transmission is not higher than 60% and can be much lower (the transmission is defined as the ratio of the on axis beam densities at the skimmer entrance to its base density). The densities are those generated at a distance of 200 mm from a high-pressure (100 bar) pulsed nozzle with 0.2 mm and a 50° conical nozzle.

Figure 12 shows the effect of the edge sharpness of the skimmer. It is recognized that skimmers have to be sharp, but how sharp do they have to be? Our simulations show that an edge sharpness of 3 μm is required to eliminate the heat soaking effects of the gas passing through the skimmer. A blunt (100 μm edge) skimmer can cause a rise of 100 K in the beam that affects the beam spread upon leaving the skimmer and may harm fragile clusters that can be in the beam. As can be seen from Figure 12, there are still collisions in the beam, even at a large distance of

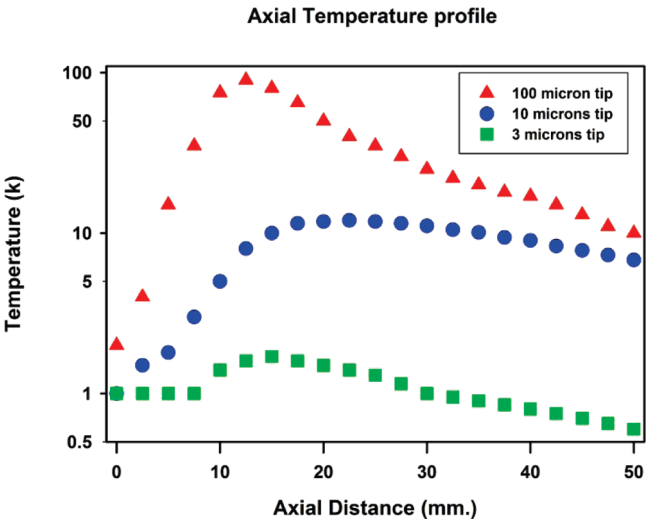

Figure 12. Axial translational temperature profile of the gas in the skimmer. The gas gets heated and compressed at the skimmer entrance, and further expansion cools it down again. Axial distance origin is 10 mm ahead of the skimmer tip. Simulations are for densities generated at a distance of 200 mm from a high-pressure (100 bar) pulsed nozzle with 0.2 mm and 50° conical nozzle. Wall thickness (in μm) at the skimmer tip is indicated.

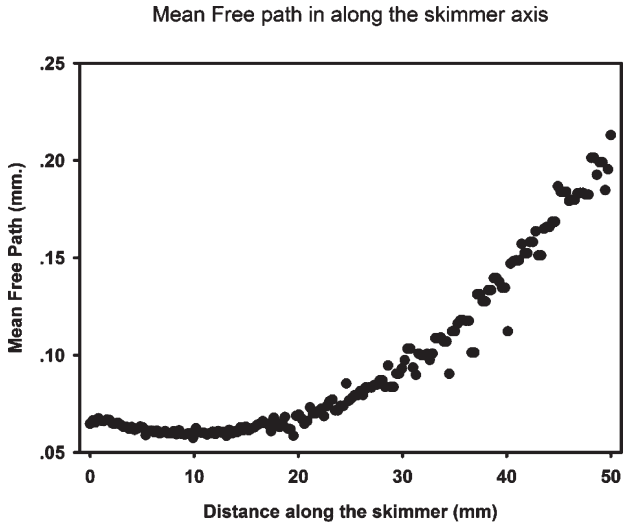

Figure 13. Mean free path along the skimmer axis. The origin is at 10 mm ahead of the skimmer tip.

200 mm from the nozzle. In fact, the simulation can calculate the mean free path along the skimmer axis, shown in Figure 13. Using this data, we can calculate that, on an average, each atom goes through about 600 collisions in its passage through the skimmer, and that the beam continues to expand and cool.

V. CONCLUSIONS

Using both simulations and measurements, we could quantify notions that are known to practitioners in the field of building supersonic beam machines. We could prove that (1) collimated beams can be produced by simple conical nozzles attached to a pulsed valve; (2) the optimal range of opening angles for best beam densities is 40−60° (full angle); (3) the produced beam densities are higher by an order of magnitude than the densities produced by a simple pinhole (sonic) nozzle; (4) the resulting high beam densities require the use of a large diameter entrance hole in the skimmers, an easy requirement when using a pulsed valve with its reduced background pressure; (5) Even with a large opening, the skimmers have to be placed at a large distance from the nozzle (~1000 nozzle diameters) to prevent skimmer clogging; (6) the beam leaving the skimmer is still expanding radially (at around 0.1 Steradians) because of its finite temperature and the radial velocities in the beam; and (7) skimmer interference (in beam temperature and transmission) can be quite severe in high densities beams (reduction in axial beam density by a factor of 10 or more).

■ ACKNOWLEDGMENT

Authors would like to thank the GIF project (I-863-37.5) and the James Franck program for partial financing. W.C. also acknowledges financial support from the Deutsche Forschungsgemeinschaft (Grant CH262/5).

■ REFERENCES

(1) Fraser, R. G. J. *Molecular Rays*; Cambridge University Press: Cambridge, 1931.
(2) Haberland, H. *Clusters of Atoms and Molecules*; Springer-Verlag: Berlin, 1994.
(3) Pauli, H. *Atoms, Molecules, and Cluster Beams I*; Springer-Verlag: Berlin, 2000; Vol. 28.
(4) Scoles, G. *Atomic and Molecular Beam Methods*; Oxford University Press: New York, Oxford, 1988; Vol. 1.
(5) Campargue, R. *J. Chim. Phys. Phys. Chim. Biol.* **1980**, *77*, R15.
(6) Hagena, O. F.; Obert, W. *J. Chem. Phys.* **1972**, *56*, 1793.
(7) Smalley, R. E.; Wharton, L.; Levy, D. H. *Acc. Chem. Res.* **1977**, *10*, 139.
(8) Toennies, J. P.; Winkelman, K. *J. Chem. Phys.* **1977**, *66*, 3965.
(9) Gentry, W. R.; Giese, C. F. *Rev. Sci. Instrum.* **1978**, *49*, 595.
(10) Otis, C. E.; Johnson, P. M. *Rev. Sci. Instrum.* **1980**, *51*, 1128.
(11) Even, U.; Bahat, D.; Cheshnovsky; Lavie, N.; Magen, Y. *J. Phys. Chem.* **1987**, *91*, 2460.
(12) Hagena, O. F. *Z. Ang. Phys.* **1963**, *16*.
(13) Murphy, H. R.; Miller, D. R. *J. Phys. Chem.* **1984**, *88*, 4474.
(14) Braun, J.; Day, P. K.; Toennies, J. P.; Wittec, G.; Neher, E. *Rev. Sci. Instrum.* **1997**, *68*, 3001.
(15) Semushin, S.; Malka, V. *Rev. Sci. Instrum.* **2001**, *72*, 2961.
(16) *The Effect of Nozzle Geometry on Cluster Formation in Molecular Beam Sources*; McDaniels, J. T., Continetti, R. E., Miller, D. R., Eds.; American Institute of Physics: New York, 2003; Vol. 23rd International Symposium.
(17) Bailey, A. B.; Dawbarn, R.; Busby, M. R. *J. AIAA* **1976**, *14*, 91.
(18) Bird, G. A. *Phys. Fluids* **1976**, *19*, 1486.
(19) Campargue, R. *J. Phys. Chem.* **1984**, *88*, 4466.
(20) Jordan, D. C.; Barling, R.; Doak, R. B. *Rev. Sci. Instrum.* **1999**, *70*, 1640.
(21) Irimia, D.; Dobrikov, D.; Kortekaas, R.; Voet, H.; Ende, D. A. v. d.; Groen, W. A.; Janssen, M. H. M. *Rev. Sci. Instrum.* **2009**, *80*, 113303.
(22) Luria, K.; Lavie, N.; Even, U. *Rev. Sci. Instrum.* **2009**, *80*, 104102.
(23) Even, U.; Al-Hroub, I.; Jortner, J. *J. Chem. Phys.* **2001**, *115*, 2069.
(24) Holmegaard, L.; Nielsen, J. H.; Nevo, I.; Stapelfeldt, H.; Filsinger, F.; Küpper, J.; Meijer, G. *Phys. Rev. Lett.* **2009**, *102*, 023001.
(25) Christen, W.; Rademann, K.; Even, U. *J. Chem. Phys.* **2006**, *125*, 174307.
(26) Hillenkamp, M.; Keinan, S.; Even, U. *J. Chem. Phys.* **2003**, *118*, 8699.

(27) Bird, G. http://www.gab.com.au/.
(28) Bird, G. A. *Molecular Gas Dynamics and the Direct Simulation of Gas Flows*; OUP: Oxford, 1994.
(29) Selden, N.; Gimelshein, N.; Gimelshein, S.; Ketsdever, A. *Phys. Fluids* **2009**, *21*, 073101.
(30) Gentry, W. R.; Giese, C. F. *Rev. Sci. Instrum.* **1975**, *46*, 104.
(31) Even, U.; Jortner, J.; Noy, D.; Lavie, N.; Cossart-Magos, C. *J. Chem. Phys.* **2000**, *112*, 8068.